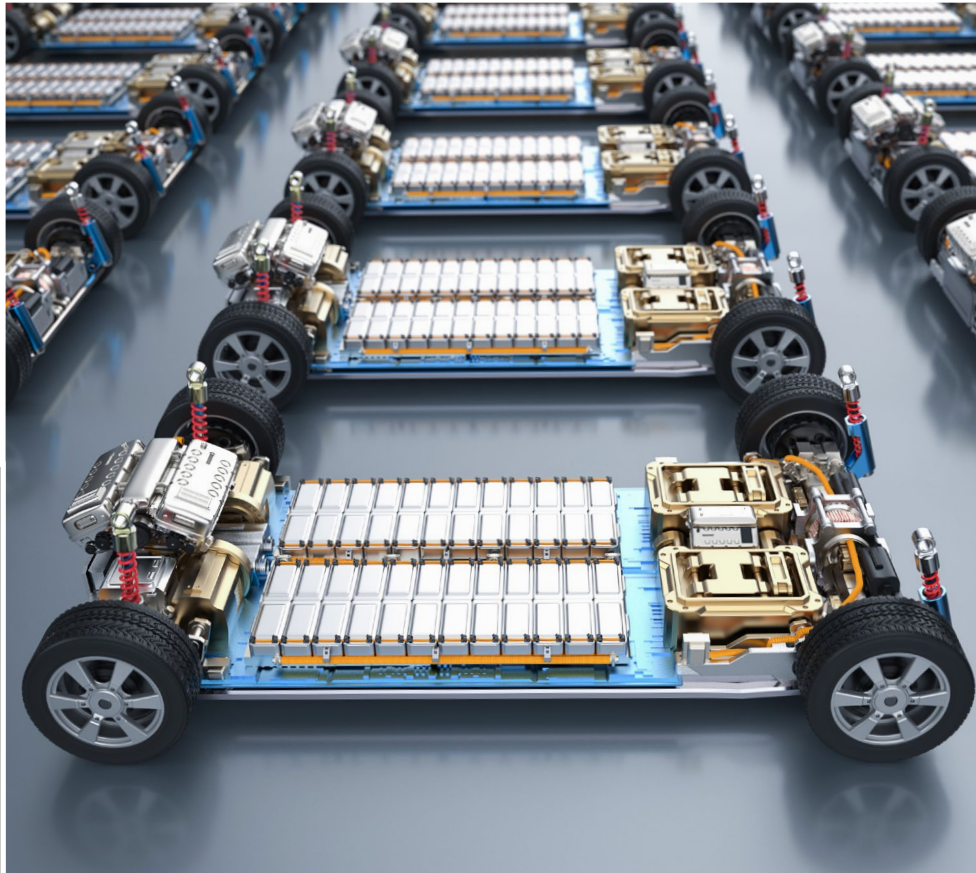
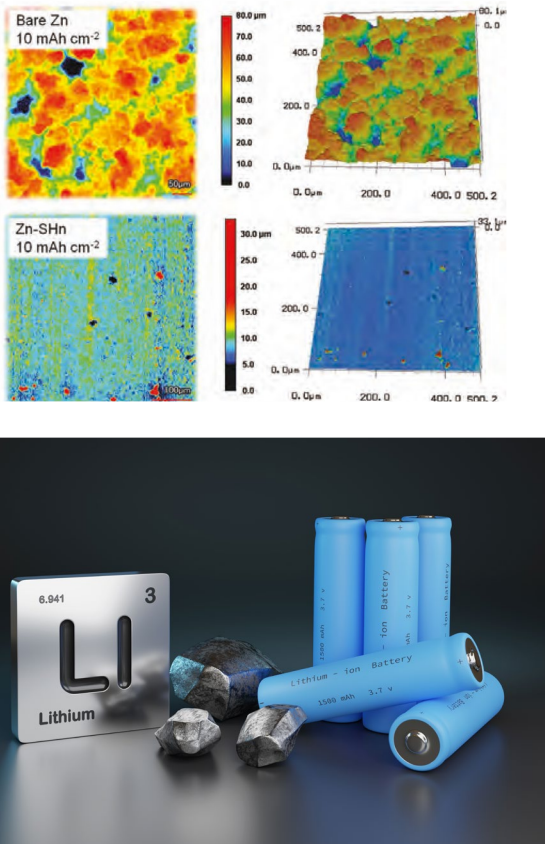


Exploring Advanced Battery Technologies

Powering the Future



Contents

3 Introduction:
Exploring Advanced Battery Technologies:
Powering the Future

6 3D-Printed Multi-Channel Metal Lattices Enabling
Localized Electric-Field Redistribution for Dendrite-Free
Aqueous Zn Ion Batteries
Adapted from Zhang, G. et. al., 2021

9 Anion Immobilization Enabled by Cation-Selective
Separators for Dendrite-Free Lithium Metal Batteries
Adapted from Zhao, Q. et. al., 2022

12 Stable Zinc Anodes Enabled by a Zincophilic
Polyanionic Hydrogel Layer
Adapted from Yang, J-L. et. al., 2022

15 Further Reading

16 About the Sponsor: Seeing is Solving

Imprint

© Wiley-VCH GmbH
Boschstr. 12,
69469 Weinheim, Germany
Email: info@wiley-vch.de
Editors: Dr. Cecilia Kruszynski
& Róisín Murtagh

Exploring Advanced Battery Technologies: Powering the Future

Modern life entails an ever-expanding demand for energy consumption. Historically, modernity has been fueled by the combustion of fossil fuels and carbon, finite resources that have not only caused substantial environmental issues but have also contributed to global warming. The primary challenge confronting our society is to transition to alternative energy sources that are both environmentally and health friendly. In response, alternative energy research has flourished, giving rise to new industries, including hydroelectric, solar, geothermal, wind, nuclear, and biomass energy.

ENERGY CONSUMPTIONS AND NEEDS

Concurrently with the expansion of renewable energy sectors, there has been a corresponding advancement in energy conversion and storage techniques. The characteristics of these emerging power generation methods have spurred the innovation and creation of diverse battery technologies – electrochemical energy storage devices that can collect and discharge energy through reversible chemical reactions.

At the forefront of battery development stands the lithium-ion battery (LIB), which first entered commercial markets in 1991. LIBs have undisputedly dominated the market and have become integral to our daily lives, seamlessly integrated into most electronic devices, from smartphones to electric vehicles.

WORKING PRINCIPLE

The working principle of a battery is based on a reduction/oxidation chemical reaction. In simple terms, there is an exchange of electrons between two poles, causing a change in the oxidation state of the involved materials. Both poles are immersed in an electrolyte, and each one reacts differently: the negative pole (anode) is oxidized due to the release of electrons, while the positive pole (cathode) is reduced due to the gaining of electrons.

This electron transfer occurs from the anode to the cathode through the circuit that needs to be powered. Ultimately, the cathode becomes full of electrons and is reduced, while the anode is oxidized. This process can be reversed by an external energy source, which is the process of charging the battery.

TYPES OF ADVANCED BATTERIES

There are various types of batteries based on their construction, with the main classification being between disposable and rechargeable batteries. As mentioned earlier, the most widely used rechargeable batteries are LIBs due to their high efficiency. LIBs can store a substantial amount of energy, and have an extended charge and discharge cycle, providing prolonged autonomy to devices. Additionally, LIBs are lighter than other rechargeable batteries of the same size, and their lifespan can range from 2 to 10 years.

Another type of battery gaining interest for its many advantages is aqueous zinc-ion batteries (ZIBs). Numerous claims have been made about the potential of ZIBs to replace LIBs, optimizing both charge density and manufacturing costs [1,2]. These batteries utilize Zn as the anode material and, similar to LIBs, operate through intercalation. This means that the same ion reacts at both the anode and cathode, traveling between the two through a liquid electrolyte.

During discharge, the anode releases an ion into the electrolyte simultaneously as the cathode absorbs it, and this process is reversed during charging.

Zinc-ion batteries present an improvement in the manufacturing processes compared to lithium batteries. Lithium's violent reactivity with water requires many production steps to be conducted in a highly controlled atmosphere, making the process costlier and more complicated. As water-based batteries, zinc-ion batteries do not face this restriction. Aqueous zinc-ion batteries (AZIBs) show promise for next-gen energy storage due to their safety, low cost, and non-toxicity [3]. In comparison to other battery technologies, AZIBs demonstrate advantages, such as high energy density, stable operation, environmental friendliness, economic viability, and simple assembly.

MAIN CHALLENGES

The limited reserves and increasing prices of Li resources restrict their application in large-scale settings. Additionally, LIBs face safety hazards due to the explosive nature of organic electrolytes and the high cost of battery raw materials. Recently, extensive efforts have been undertaken to address these issues, including the design of anode and cathode structures, the development of new cathode materials, the optimization of electrolyte components, and the modification of current collectors [4].

Another significant challenge is that lithium metal anodes often experience shortened lifecycles marred by the formation of lithium dendrites during battery operation. The overgrown dendritic lithium poses a risk of short-circuiting the battery by penetrating the routine separator, leading to serious security incidents.

Dendrite formation is a common issue for both LIBs and ZIBs [5,6]. Dendrites are thin, tentacle-like metal filaments that develop on the battery electrode during charge and discharge cycles. Different topologies of Li and Zn dendrites infiltrate the electrolyte, causing problems, such as short circuits, overheating, and even fires. These formations can puncture the separator which prevents contact between the cathode and anode. Moreover, they escalate unwanted reactions between the electrolyte and the metal, accelerating battery failure.

In addition to dendrite growth, ZIBs also face challenges, such as cathode dissolution,

electrolyte decomposition, hydrogen evolution, by-products, and corrosion issues. These problems lead to diminished electrochemical performance and even short circuits.

RESEARCH

Current issues in LIBs and ZIBs, as well as in other systems, are under extensive study, with diverse strategies being proposed. The primary focus of current research lies in the optimization of anode, cathode, and electrolyte materials [4–6].

For instance, Zhao *et al.* [7] introduced a novel polyvinylidene fluoride (PVDF) cation-selective separator to immobilize anions within the liquid electrolyte of a LIB. The construction of a dendrite-free Li anode was the key objective, and the separator, fabricated through a simple doctor-blading process of PVDF, exhibited outstanding performance.

In another approach, Zhang *et al.* [8] addressed the challenge of dendrite formation by exploring the construction of a 3D high-surface-area zinc anode. Increased surface area in a 3D conductive host helped reduce local current density and ensured a uniform distribution of interfacial charge. The authors combined 3D printing with electroless deposition to fabricate a conductive 3D nickel lattice (3D Ni) current collector. Subsequently, they achieved homogeneously electrodeposited Zn on the 3D Ni surface, resulting in the formation of 3D Ni-Zn lattices (3D Ni-Zn) as the anode for ZIBs. They successfully inhibited Zn dendrite formation in the 3D Ni-Zn anode, leading to a significant improvement in the electrochemical performance of batteries.

A different strategy was adopted by Yang *et al.* [9] to alleviate the problem of dendrite growth. They created a protective layer or solid electrolyte interphase (SEI) on the Zn electrode, preventing direct contact of Zn with water and inhibiting dendrite formation. They developed a polyanionic hydrogel SEI layer with multiple functionalities, demonstrating strong hydrogel-solid adhesion. This innovative hydrogel film served as an effective artificial protective layer for the Zn-metal anode. Consequently, the strategy of constructing a stable ionically conductive hydrogel-Zn interface with regulated Zn nucleation proved highly effective. The researchers anticipate that this approach could be a versatile protection method for metal electrodes across various battery systems.

CONCLUSION

The evolution of battery technologies plays a pivotal role in meeting the demands of the ever-growing need for energy consumption. LIBs have been instrumental in powering electronic devices, but their limitations, such as safety concerns and resource constraints, have led to a surge in research for advanced alternatives.

The challenges associated with LIBs and ZIBs, particularly dendrite formation, pose significant hurdles in achieving reliable and safe energy storage solutions. Addressing these challenges requires innovative strategies, as demonstrated by recent research efforts. Novel materials, protective layers, and advanced anode and cathode structures have been proposed to enhance battery performance and safety.

The ongoing research efforts to optimize anode, cathode, and electrolyte materials exemplify a steadfast dedication to surmounting current constraints, ultimately forging a path toward more sustainable energy storage solutions. As we delve deeper into the complexities of advanced battery technologies, the collective efforts of researchers worldwide showcase a commitment to powering the future with efficient, safe, and environmentally friendly energy storage systems. The journey towards unlocking the full potential of batteries continues, propelling us closer to a sustainable and resilient energy future.

Are you fascinated by the groundbreaking advancements in battery research?

Uncover the secrets of the latest innovations and discoveries in our previous exclusive eBook:

The Impact of Lithium-Ion Batteries on Renewable Energy: From Prototype to Commercial Success

References

- [1] Song, M. et al. (2018). Recent Advances in Zn-Ion Batteries. *Advanced Functional Materials*. DOI: [10.1002/adfm.201802564](https://doi.org/10.1002/adfm.201802564).
- [2] Aizudin, M. et al. (2024). Recent Advancements of Graphene-Based Materials for Zinc-Based Batteries: Beyond Lithium-Ion Batteries. *Small*. DOI: [10.1002/smll.202305217](https://doi.org/10.1002/smll.202305217).
- [3] Zhang, X. et al. (2024). Smart Aqueous Zinc Ion Battery: Operation Principles and Design Strategy. *Advanced Science*. DOI: [10.1002/advs.202305201](https://doi.org/10.1002/advs.202305201).
- [4] Ma, L. et al. (2024). Current challenges and progress in anode/electrolyte interfaces of all-solid-state lithium batteries. *eTransportation*. DOI: [10.1016/j.etrans.2024.100312](https://doi.org/10.1016/j.etrans.2024.100312).
- [5] Yang, Q. et al. (2020). Dendrites in Zn-Based Batteries. *Advanced Materials*. DOI: [10.1002/adma.202001854](https://doi.org/10.1002/adma.202001854).
- [6] Zhang, X. et al. (2019). Dendrites in Lithium Metal Anodes: Suppression, Regulation, and Elimination. *Accounts of Chemical Research*. DOI: [10.1021/acs.accounts.9b00437](https://doi.org/10.1021/acs.accounts.9b00437).
- [7] Zhao, Q. et al. (2022). Anion Immobilization Enabled by Cation-Selective Separators for Dendrite-Free Lithium Metal Batteries. *Advanced Functional Materials*. DOI: [10.1002/adfm.202112711](https://doi.org/10.1002/adfm.202112711).
- [8] Zhang, G. et al. (2021). 3D-Printed Multi-Channel Metal Lattices Enabling Localized Electric-Field Redistribution for Dendrite-Free Aqueous Zn Ion Batteries. *Advanced Energy Materials*. DOI: [10.1002/aenm.202003927](https://doi.org/10.1002/aenm.202003927).
- [9] Yang, J. et al. (2022). Stable Zinc Anodes Enabled by a Zincophilic Polyanionic Hydrogel Layer. *Advanced Materials*. DOI: [10.1002/adma.202202382](https://doi.org/10.1002/adma.202202382).

01 3D-Printed Multi-Channel Metal Lattices Enabling Localized Electric-Field Redistribution for Dendrite-Free Aqueous Zn Ion Batteries

Adapted from Zhang, G. et. al., 2021

Rechargeable zinc ion batteries are regarded as a preferable candidate for next-generation energy storage systems owing to their merits of environmental benignity, low cost, and high safety. Here, a novel 3D Zn metal anode with multi-channel lattice structures employing the combined 3D printing and electroless plating/electroplating techniques is reported.

INTRODUCTION

Advances in portable electronics, electric vehicles, and grid energy storage drive the demand for reliable energy storage. Aqueous rechargeable zinc-ion batteries (ZIBs) are favored for their environmental friendliness, low cost, and high safety [1]. However, challenges like dendrite growth and side reactions of the zinc anode hinder widespread adoption. Zinc dendrites can pierce separators, causing short circuits. Traditional conductive hosts promote dendrite formation due to their low surface area. Constructing a 3D high-surface-area zinc anode helps inhibit dendrite formation, but pure zinc 3D sponge electrodes suffer structural damage during repeated cycles. Additionally, zinc anodes obtained through various methods may hinder ion diffusion and create void spaces without zinc deposition [2]. To address these issues, we proposed a strategy involving 3D printing and electroless deposition to create a conductive 3D nickel lattice (3D Ni) current collector.

RESULTS AND DISCUSSION

Specially designed 3D polymer lattices, printed with a high-precision PμSL 3D printer (10 μm accuracy), undergo modification

treatments (KMnO_4 solution immersion and oxygen plasma cleaning) to enhance polymer wettability before metallization. Ni is selected for metallized coating [3]. Conductive 3D Ni lattices are produced via electroless deposition and electrodeposition. After metallization, a uniform Ni layer coats the 3D polymer, forming conductive networks. To boost electrical conductivity, a second Ni layer is electrodeposited. The resulting 3D Ni-Zn lattices, featuring a real 3D structure and rigid supporting skeleton, are fabricated through electrodeposition of Zn on 3D Ni surfaces.

The 3D Ni composition includes C, O (from the 3D polymer framework), and P (from Ni-P alloy coating via electroless deposition). Zn is evenly deposited on both internal and external surfaces of the 3D Ni skeleton.

Coulombic efficiency (CE), a vital parameter for Zn plating/stripping reversibility, is evaluated. In a 3D Ni//Zn foil cell, CE remains stable over 350 cycles at 10 mA cm^{-2} with a 1 mA h cm^{-2} capacity, attributed to inhibited side reactions and dendrite growth. Conversely, 2D Ni//Zn foil cell CEs fluctuate after approximately 40 cycles, indicating unstable Zn plating/stripping on the 2D Ni substrate.

To grasp the Zn plating and stripping principles in 2D/3D electrodes, Figure 1a-d illustrates simulations of current density distribution. The distinctiveness of 3D Ni-Zn electrode lies in its enlarged specific area and minimized Zn nucleation size [4]. Examining the current density vectors reveals the direction of current flow, with vector color and length proportional to current density. In 2D Ni-Zn electrode (Figure 1b), tips formed during nucleation induce the “tip effect,” fostering Zn dendrite growth and dead zinc formation, leading to capacity deterioration. Conversely, 3D Ni-Zn electrode (Figure 1d) with an interconnected lattice regulates zinc deposition, altering growth direction and preventing separator penetration.

Simulated zinc ion concentration during deposition highlights the advantages of 3D Ni-Zn over 2D Ni-Zn. The multi-channel structure redistributes current flow, enhancing zinc ion attraction. A 1D-concentration profile along the Y direction shows lower Zn-ion concentration near the upper surface of 2D Ni-Zn, leading to increased concentration polarization. At high current density, 2D Ni-Zn intensifies concentration polarization, promoting fast Zn dendrite growth due to elevated ionic flux near growing tips [5].

Uniform current density ensures even Zn^{2+} adsorption on the electrode surface. Surfaces of 2D Ni-Zn and 3D Ni-Zn electrodes cycled in symmetrical cells are examined using a high-magnification optical microscope with a 3D scanner. Figure 1e displays the rough surface of the cycled 2D Ni-Zn electrode. The corresponding 3D height image (Figure 1g) reveals a 248 μm height difference, indicating Zn dendrites capable of penetrating the separator. In contrast, the cycled 3D Ni-Zn electrode displays a flat surface without dendrites (Figure 1f). Notably, its height difference is less than 50 μm (Figure 1h), significantly lower than the 2D Ni-Zn, showcasing the effective inhibition of dendrite growth by the 3D multi-channel lattice structure.

To assess the practical application of the 3D Ni-Zn anode, a full cell is assembled with a polyaniline-intercalated vanadium oxide (PVO) cathode. The PVO//3D Ni-Zn battery exhibits lower voltage polarization (approx. 52 mV) compared to the PVO//2D Ni-Zn battery,

confirming superior reversibility attributed to the 3D lattice structure. Examining rate performance, the PVO//3D Ni-Zn battery consistently outperforms the PVO//2D Ni-Zn battery, showcasing higher average discharge capacity across the entire current range.

Post-long-term cycling disassembled full cells reveal electrode morphology and composition changes. The 2D Ni-Zn electrode exhibits disorderly zinc flakes, indicating uncontrolled Zn dendrite growth. In contrast, the outer surface of the 3D Ni-Zn electrode remains compact without mossy-like dendrites, resembling the fresh electrode. The 3D Ni-Zn lattice electrode encourages homogeneous Zn deposition into microchannels, preventing dendrite growth on the outer surface.

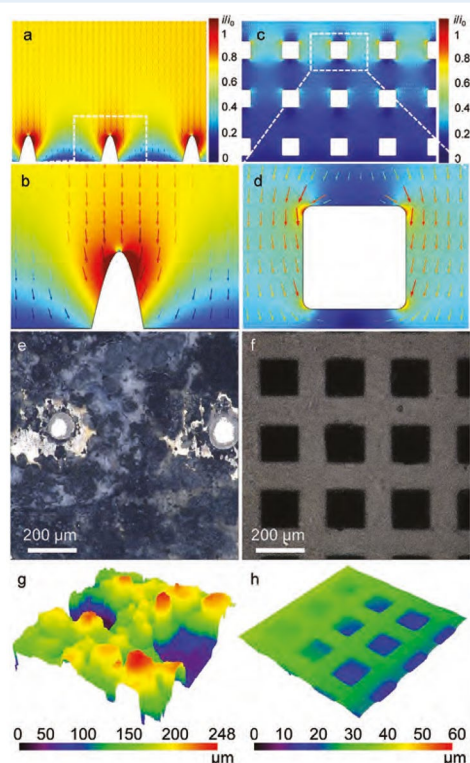


Figure 1. Simulations of the relative intensity distributions of localized electric field for a, b) 2D Ni-Zn electrode and c, d) 3D Ni-Zn electrode. The high-magnification optical images and corresponding 3D height images for the surfaces of e, g) 2D Ni-Zn and f, h) 3D Ni-Zn electrodes after cycling.

CONCLUSION

We developed a dendrite-free 3D Ni–Zn anode for aqueous ZIBs using 3D printing and electroless/electrodeposition. Simulations on current density distribution reveal that the multi-channel lattice structure improves electric field distribution, ensuring uniform zinc deposition, as validated by *in situ* optical microscope observation. Consequently, the 3D Ni–Zn anode effectively prevents Zn dendrite formation, significantly enhancing battery electrochemical performance. The successful creation of a PVO/Zn battery holds promise for next-gen energy storage devices.

EXPERIMENTAL SECTION

A typical electroless deposition method was used to synthesize nickel–phosphorus metal layer on the surface of the previous 3D sample to make it conductive. The conductive lattices

were used as working electrode and the deposition process was conducted at a constant voltage of 2.0 V for 6 min. Then, Zn was electrodeposited on the conductive 3D Ni electrode. The mass loading of zinc was 6.02 mg cm⁻².

The layered PVO was synthesized by a typical procedure. The super depth surface profile measurement microscope (Olympus DSX1000) was used to get the high-magnification optical images and 3D height images.

The homemade visual cells were assembled with 3D Ni electrode and Zn foil or 2D Ni electrode and Zn foil. Cyclic voltammetry (CV) curves were conducted using an electrochemical workstation (CHI660e, China). Galvanostatic charge/discharge curves and long-term cycling tests were recorded on a CT-4008 battery testing system (Shenzhen NEWARE Co., Ltd.).

References

- [1] Zhong, S. et al. (2020). Long-aspect-ratio N-rich carbon nanotubes as anode material for sodium and lithium ion batteries. *Chemical Engineering Journal*. DOI: [10.1016/cej.2020.125054](https://doi.org/10.1016/cej.2020.125054).
- [2] Zhang, Q. et al. (2020). Interfacial Design of Dendrite-Free Zinc Anodes for Aqueous Zinc-Ion Batteries. *Angewandte Chemie International Edition*. DOI: [10.1002/anie.202000162](https://doi.org/10.1002/anie.202000162).
- [3] Zhang, Q. et al. (2019). The Three-Dimensional Dendrite-Free Zinc Anode on a Copper Mesh with a Zinc-Oriented Polyacrylamide Electrolyte Additive. *Angewandte Chemie International Edition*. DOI: [10.1002/anie.201907830](https://doi.org/10.1002/anie.201907830).
- [4] Zeng, Y. et al. (2019). Dendrite-Free Zinc Deposition Induced by Multifunctional CNT Frameworks for Stable Flexible Zn-Ion Batteries. *Advanced Materials*. DOI: [10.1002/adma.201903675](https://doi.org/10.1002/adma.201903675).
- [5] Bazant, M.Z. (1995). Regulation of ramified electrochemical growth by a diffusive wave. *Physical Review E*. DOI: [10.1103/PhysRevE.52.1903](https://doi.org/10.1103/PhysRevE.52.1903).

02 Anion Immobilization Enabled by Cation-Selective Separators for Dendrite-Free Lithium Metal Batteries

Adapted from Zhao, Q. et. al., 2022

The lithium dendrite issue is a major bottleneck that limits the utilization of lithium metal anodes in high-energy rechargeable batteries. From the perspective of the dendrite nucleation mechanism, this work develops a new type of cation-selective (CS) separator with anion immobilization behavior to boost the lithium metal anode and is anticipated to provide considerable insight for the creative design of CS separators toward dendrite-free LMBs.

INTRODUCTION

An ever-growing energy demand urgently calls for the development of rechargeable batteries with higher energy densities to extend the driving range of electric vehicles and to power portable electronic devices with increased energy consumption [1]. Lithium metal is recognized as an ideal anode material for constructing high-energy batteries because of its unprecedentedly high theoretical capacity and extremely low electrochemical potential [2]. Nevertheless, the lithium metal anode usually suffers from a shortened lifecycle caused by the lithium dendrites during the battery operation [3]. The overgrown dendritic lithium can short-circuit the battery by penetrating the routine separator and lead to serious security incidents.

The onset of dendrite nucleation can be delayed by prolonging the formation of a space-charge region near the negative electrode through immobilizing anions within the electrolyte, offering a pragmatic insight into the development of dendrite-free lithium anodes.

In a routine battery with liquid electrolyte, a separator provides an available platform to immobilize anions because it directly affects the ionic transport behavior [4]. Thus, a cation-selective (CS) separator is considered to prevent the nucleation and growth of lithium dendrite, which conducts Li^+ ions and anchors anions. The capacity of anion immobilization could be quantified by the transference number of Li^+ ion (t_{Li}^+).

We demonstrated the construction of a robust large-area CS separator based on a self-standing polyvinylidene fluoride (PVDF) membrane for boosting lithium metal anodes.

RESULTS AND DISCUSSION

Characterizations of Cation-Selective Separator

A robust large-area CS separator was obtained by taking advantage of a simple doctor-blade of PVDF coating. The as-prepared large-scaled CS separator was highly flexible and transparent. The separator had a uniform and thin thickness of $\approx 16.1 \mu\text{m}$, the porosity was below 5%,

and it had an electrolyte uptake rate of 340% (ca. three times higher than that of the Celgard separator). The CS separator could maintain no heat shrinkage deformation up to 140 °C (284 °F).

A concentration diffusion test of anionic dye methyl orange demonstrates that the CS separator could effectively prevent the transmembrane diffusion of anionic dye for a long time over 48 h. For comparison, the anionic dye could easily diffuse through a commercial Celgard separator.

Then, molecular dynamics simulations were conducted to elucidate the transport behaviors of both Li^+ and PF_6^- ions within the separator. A model representing the CS separator (10 nm) sandwiched between two electrolyte layers (5 nm) was constructed. The average transport rate of Li^+ ions in the separator was 1.58 times higher than that of PF_6^- ions. Given both diffuse and ion transport processes, the contribution of Li^+ ions to the total current was 4.21 ($2.67 \times 1.58 = 4.21$) times higher than that of PF_6^- ions.

Cation-Selective Separator toward Dendrite-Free Lithium Anode

The calculated t_{Li}^+ for the CS separator and electrolyte system reached a high value of 0.81, which was much higher than that of the Celgard one (0.40). In this case, a rather

low t_{anion} (0.19) indicated an excellent anion immobilization behavior of the CS separator, which was the basis for suppressing nucleation and growth of lithium dendrites.

To demonstrate the Li metal anode stabilized by the CS separator, in situ observation of Li dendrites was conducted by optical microscope at a galvanostatic deposition of 1 mA cm⁻² (Figure 1). In the symmetric $\text{Li}|\text{Li}$ cell with Celgard separator, the Li dendrite formed on the surface of the Li metal electrode and grew rapidly as illustrated in Figure 2. The growth of dendrite was first from the tip side because the protrusion with high curvature had a considerably higher electric field distribution [1]. Then, there was a lateral growth from another tip of the dendrite. Both the morphology and volume exhibited significant changes compared with the initial state just after 3 min. For the CS separator-based cell, the Li metal electrode kept a quite smooth and dendrite-free surface during a long-term Li deposition of 60 min. In the battery with routine Celgard separator, the LiF was not easy to form on the Li anode. While, the CS separator demonstrated excellent anion immobilization capability, which could stabilize the F-containing anions on the surface of the Li anode and promote the formation of LiF in the SEI. In this case, the surface of cycled Li foil from the Celgard cell became quite rough and lost the metallic luster, which was ascribed to the formation of massive Li dendrites.

Figure 1. Experimental set-up of the optical cell for *in situ* observation of Li dendrite growth and the obtained optical image of separator sandwiched between two Li foils. During the measurement, the separator was sandwiched between two Li foils, which were placed perpendicular to the glass view window in the optical cell. The two electrodes were respectively connected with the Li foils for the electrochemical measurement.

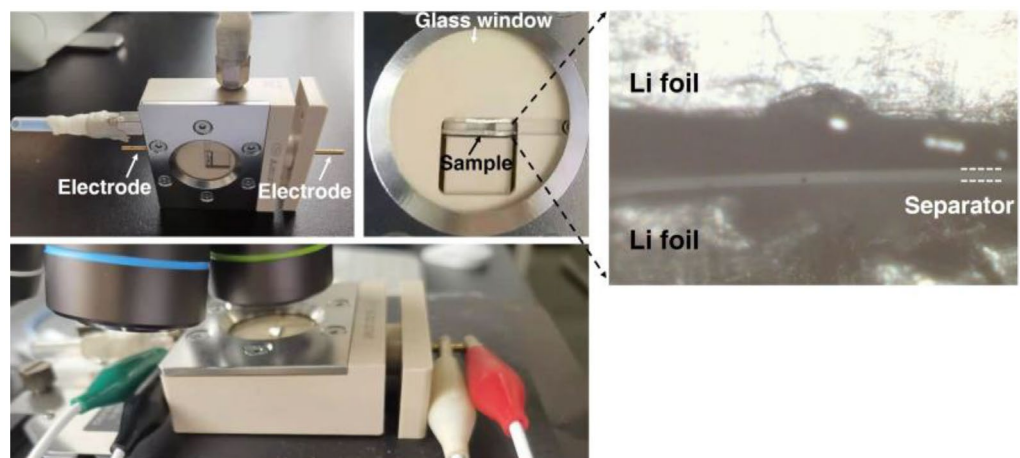
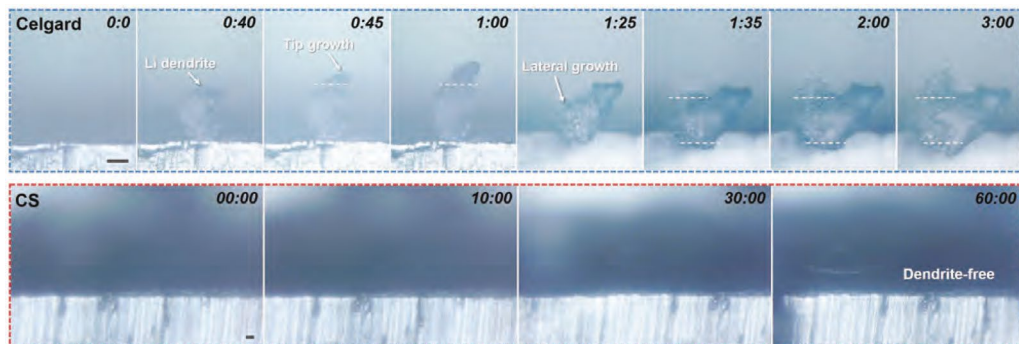


Figure 2. Cation-selective separator suppressing Li dendrite growth. a) *In situ* observation of Li dendrites growth on the surface of Li metal with CS/Celgard separators on top sides at a galvanostatic deposition of 1 mA cm^{-2} . Scale bars are $20 \mu\text{m}$. The time increments for the images are seconds



Cation-Selective Separator Boosting Lithium Metal Battery

Benefiting from the suppression of Li dendrites, the CS separators were further assembled into LiFePO_4 -based LMBs to study the electrochemical energy storage performances.

The battery integrated with the CS separator could deliver a discharge capacity of 135.8 mAh g^{-1} at 0.1 C , which was a 10.6% improvement over the battery based on the Celgard separator ($122.75 \text{ mAh g}^{-1}$). At a high rate of 1.0 C , the discharge capacity of the CS separator-based battery was also higher than that of the Celgard separator.

CONCLUSION

The separator obtained from simple doctor-blading of PVDF demonstrated excellent CS performance, in which the Li^+ transference number reached a high value of 0.81. Implementation of CS separators

into LMBs led to an improvement in the overall electrochemical performance including discharge capacity, rate capability, and cycling durability. This work provided an effective strategy for the construction of dendrite-free LMBs.

EXPERIMENTAL SECTION

The CS separators were prepared using a classical doctor-blade method. The pore-creating in the CS separator was based on the classical nonsolvent-induced phase separation method [5]. *In situ* observation of Li dendrites was conducted using an *in situ* electrochemical cell coupled with an optical microscope (Olympus, BX53). The ionic transport behavior of the CS separators was studied in symmetric $\text{Li}|\text{separator}|\text{Li}$ cells. Commercial polypropylene separators (Celgard 2400, USA) served as control groups. The molecular dynamics simulations in this work were performed using the GROMACS (version 2018.4) software package [6].

References:

- [1] Lin, D. et al. (2017). Reviving the lithium metal anode for high-energy batteries. *Nature Nanotechnology*. DOI: [10.1038/nnano.2017.16](https://doi.org/10.1038/nnano.2017.16).
- [2] Guo, Y. et al. (2017). Reviving Lithium-Metal Anodes for Next-Generation High-Energy Batteries. *Advanced Materials*. DOI: [10.1002/adma.201700007](https://doi.org/10.1002/adma.201700007).
- [3] Cheng, X.-B. et al. (2017). Toward Safe Lithium Metal Anode in Rechargeable Batteries: A Review. *Chemical Reviews*. DOI: [10.1021/acs.chemrev.7b00115](https://doi.org/10.1021/acs.chemrev.7b00115).
- [4] Liu, K.-L. et al. (2019). A novel non-porous separator based on single-ion conducting triblock copolymer for stable lithium electrodeposition. *Journal of Power Sources*. DOI: [10.1016/j.jpowsour.2019.02.048](https://doi.org/10.1016/j.jpowsour.2019.02.048).
- [5] Kuo, C.-Y. et al. (2008). Fabrication of a high hydrophobic PVDF membrane via nonsolvent induced phase separation. *Desalination*. DOI: [10.1016/j.desal.2007.09.025](https://doi.org/10.1016/j.desal.2007.09.025).
- [6] Hess, B. et al. (2008). GROMACS 4: Algorithms for Highly Efficient, Load-Balanced, and Scalable Molecular Simulation. *Journal of Chemical Theory and Computation*. DOI: [10.1021/ct700301q](https://doi.org/10.1021/ct700301q).

03 Stable Zinc Anodes Enabled by a Zincophilic Polyanionic Hydrogel Layer

Adapted from Yang, J-L. et al., 2022

The practical application of the Zn-metal anode for aqueous batteries is greatly restricted by catastrophic dendrite growth, intricate hydrogen evolution, and parasitic surface passivation. Herein, a polyanionic hydrogel film is introduced as a protective layer. This strategy paves a new way for future Zn-anode design and safe aqueous battery construction.

INTRODUCTION

Aqueous zinc-ion batteries (AZIBs) are promising for next-gen energy storage due to their safety, low cost, and non-toxicity [1,2]. Investigated extensively for their high theoretical capacities, AZIBs face challenges, notably uncontrolled Zn dendrite formation leading to inner shorts and fire risks [3]. Additionally, brittle Zn dendrites result in “dead Zn,” causing material loss. Thermodynamically unstable Zn in aqueous solutions triggers hydrogen evolution reactions (HER), accumulating insulating Zn²⁺ byproducts that hinder redox kinetics and coulombic efficiency, and induce uneven Zn deposition [4].

Addressing the mentioned issues involves proposing various strategies to protect the Zn anode, such as modifying the Zn surface and adjusting electrolyte composition [5]. Zn surface modification aims to create a protective layer or solid electrolyte interphase (SEI) to impede direct Zn-H₂O contact and hinder dendrite growth. However, these protective layers only partially alleviate some issues. An ideal SEI for Zn protection must simultaneously exhibit high Zn²⁺ conductivity, moderate mechanical properties, low electronic conductivity, and strong interfacial contact with Zn metal. This work aims to develop a novel polyanionic hydrogel SEI layer to fulfill these multiple requirements.

RESULTS AND DISCUSSION

Mechanically polished Zn plates underwent silane-coupling agent (3-methacryloxypropyltrimethoxysilane - MPS) treatment, grafting functional silanes on the Zn surface. The pre-hydrogel solution, containing 2-acrylamido-2-methyl-1-propane-sulfonic acid sodium salt (AMPS) and acrylamide (AAm), was applied to the Zn-S surface. Post-polymerization, a polyanionic hydrogel with negatively charged $-\text{SO}_3^-$ groups formed on the Zn surface (denoted as Zn-SHn). Surface characterization confirmed successful AMPS-induced $-\text{SO}_3^-$ groups, crucial for multiple functions.

To highlight the silane-coupling agent's role, Zn-SHn and Zn-Hn were immersed in 2 m ZnSO₄ electrolyte for 5 days. The silane-treated hydrogel layer remained unchanged, while the hydrogel layer on Zn-Hn tended to peel off.

Avoiding direct exposure to water molecules due to Zn-O bonding, it was suggested that the polyanionic hydrogel could suppress hydrogen evolution reaction (HER) at the anode. Corrosion potentials showed a negligible positive shift for Zn-S and Zn-Hn, with corrosion currents close to bare Zn (4.84 mA cm⁻² on Zn-S, 5.76 mA cm⁻² on Zn-Hn), indicating only reinforced hydrogel-Zn interfaces stabilized the Zn surface.

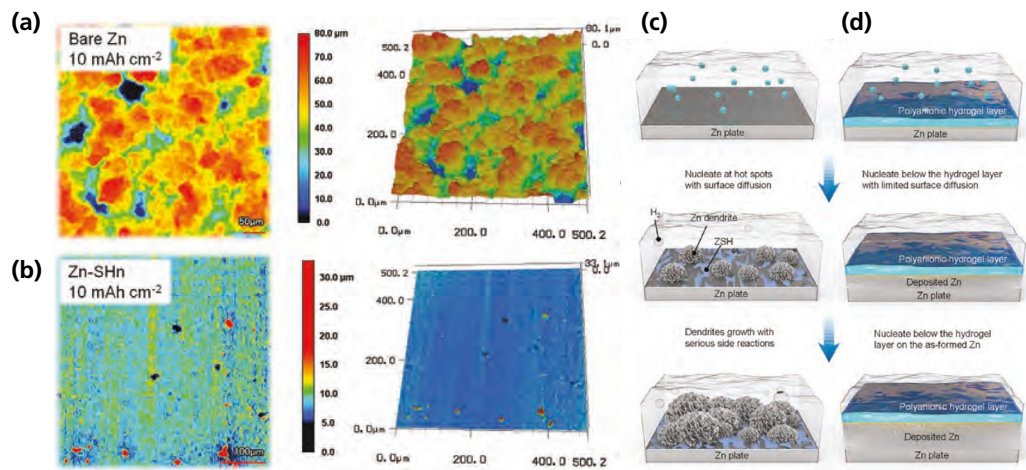


Figure 1. Zn nucleation and dendrites growth behaviors. (a,b) CLSM images of bare Zn (a) and Zn-SHn (b) electrodes after Zn deposition. (c,d) Schematics of the Zn precipitation on bare Zn (c) and Zn-SHn (d) surface.

Hydrogen evolution current density on Zn-SHn was 23 mA cm^{-2} at -2.2 V (vs saturated calomel electrode), lower than bare Zn (53 mA cm^{-2}), Zn-S (41 mA cm^{-2}), and Zn-Hn (43 mA cm^{-2}), indicating increased difficulty in hydrogen evolution from the Zn-SHn electrode surface [6].

Brittle $\text{Zn}_4\text{SO}_4(\text{OH})_6 \cdot x\text{H}_2\text{O}$ (ZSH), a primary HER byproduct causing local pH increase, was minimized by the hydrogel layer. Removal of the top hydrogel layer revealed negligible ZnSH on the Zn surface. The hydrogel layer retained its state after 5 days, while bare Zn displayed a rough surface with flake-shaped byproducts. The robust adhesion of the polyanionic hydrogel to the strengthened hydrogel-Zn interface efficiently suppressed HER in aqueous electrolyte, preventing Zn surface passivation.

Evaluating Zn nucleation and dendrite growth, at a 10 mAh cm^{-2} Zn plating capacity, Zn-SHn maintained a smooth surface without dendrite formation. In contrast, bare Zn exhibited patchy spots, while Zn-SHn showed a uniform dark color, indicating more homogeneous Zn nucleation compared to bare Zn.

To depict the uniform Zn plating on Zn-SHn, electrodes post 10 mAh cm^{-2} deposition were examined with confocal laser scanning microscopy (CLSM). Figure 1a shows bare Zn with dendrites and high roughness due to limited nucleation sites. With the hydrogel layer's protection (Figure 1b), zincophilic

nucleation sites facilitate homogeneous Zn nucleation, preventing dendrite formation and maintaining the hydrogel layer's smooth state.

Analyzing Zn precipitation on bare Zn and Zn-SHn (Figure 1c,d), bare Zn suffers uneven current density and significant hydrogen evolution reaction (HER), leading to dendrite growth and byproducts passivation. In the polyanionic hydrogel presence, Zn^{2+} is captured, transported through the water-rich framework, and homogeneously nucleated beneath the hydrogel layer.

To assess Zn-SHn's viability in AZIB applications, $\text{NaV}_3\text{O}_8 \cdot 1.5\text{H}_2\text{O}$ (NVO) served as the cathode, synthesized via hydrothermal method [7]. NVO||Zn-SHn exhibited cyclic voltammetry curves akin to NVO||Zn, with slightly higher polarization due to increased Zn nucleation overpotential. Raising current density from 0.2 to 10 A g^{-1} , NVO||Zn-SHn outperformed NVO||Zn in specific capacity, indicating fast redox kinetics.

Cycle performance via galvanostatic charge/discharge revealed NVO||Zn-SHn maintaining outstanding capacity exceeding 300 mAh g^{-1} under 1 A g^{-1} , with minimal decay after 500 cycles. In contrast, NVO||Zn exhibited much lower capacity retention, reaching 250 mAh g^{-1} after 300 cycles.

To validate the polyanionic hydrogel layer's protective effect, anode morphologies

post-cycling were examined. Bare Zn became porous with flakes, while Zn-SHn remained smooth and intact. Suppressed HER on Zn-SHn reduced surface passivation, enhancing redox reversibility in full cells.

CONCLUSION

We have demonstrated that thin polyanionic hydrogel is an effective artificial protective layer for Zn-metal anode. This strategy for constructing a stable ionically conductive hydrogel–Zn interface with regulated Zn nucleation is highly effective and it is expected to be a versatile protection approach for metal electrodes in various batteries.

EXPERIMENTAL SECTION

Zn plates underwent sandpaper polishing, air plasma cleaning, and immersion in a silane coupling agent-containing aqueous solution [8]. After stirring for 4 h, the sample was cleaned with ethanol and deionized

water, resulting in Zn–S, which was dried in a vacuum oven. Next, the prehydrogel solution was applied to Zn–S plates, compressed and sealed in glass molds for comprehensive coverage. UV light (365 nm) irradiation for 4 h produced Zn plates with a polyanionic hydrogel coating. Neutral hydrogel-modified Zn (Zn–SH) was prepared similarly, using a neutral pre-hydrogel solution. Zn–Hn, denoting polyanionic hydrogel-modified Zn without the silane-coupling agent, was also prepared.

For NVO preparation, V_2O_5 and NaOH were dissolved in deionized water, stirred for 4 h, and transferred to a Teflon-lined stainless steel autoclave, where it was kept at 180 °C for 24 h. The resulting orange powder was washed with deionized water and vacuum oven-dried at 80 °C overnight.

A 3D measuring laser microscope (Olympus, LEXT OLS5000) facilitated laser confocal scanning microscopy (LCSM) image acquisition for samples after Zn deposition.

References

- [1] Jia, X. et al. (2020). Active Materials for Aqueous Zinc Ion Batteries: Synthesis, Crystal Structure, Morphology, and Electrochemistry. *Chemical Reviews*. [DOI: 10.1021/ACS.CHEMREV.9B00628](https://doi.org/10.1021/ACS.CHEMREV.9B00628).
- [2] Yan, J. et al. (2021). High-Voltage Zinc-Ion Batteries: Design Strategies and Challenges. *Advanced Functional Materials*. [DOI: 10.1002/ADFM.202010213](https://doi.org/10.1002/ADFM.202010213).
- [3] Zuo, Y. et al. (2021). Zinc dendrite growth and inhibition strategies. *Materials Today Energy*. [DOI: 10.1016/J.MTENER.2021.100692](https://doi.org/10.1016/J.MTENER.2021.100692).
- [4] Blanc, L.E. et al. (2020). Scientific Challenges for the Implementation of Zn-Ion Batteries. [DOI: 10.1016/j.joule.2020.03.002](https://doi.org/10.1016/j.joule.2020.03.002).
- [5] Yang, J. et al. (2022). Zinc Anode for Mild Aqueous Zinc-Ion Batteries: Challenges, Strategies, and Perspectives. *Nano-Micro Letters* 2022 14:1. [DOI: 10.1007/S40820-021-00782-5](https://doi.org/10.1007/S40820-021-00782-5).
- [6] Liu, H. et al. (2021). Building Ohmic Contact Interfaces toward Ultrastable Zn Metal Anodes. *Advanced Science*. [DOI: 10.1002/advs.202102612](https://doi.org/10.1002/advs.202102612).
- [7] Wan, F. et al. (2018). Aqueous rechargeable zinc/sodium vanadate batteries with enhanced performance from simultaneous insertion of dual carriers. *Nature Communications*. [DOI: 10.1038/s41467-018-04060-8](https://doi.org/10.1038/s41467-018-04060-8).
- [8] Yuk, H. et al. (2016). Tough bonding of hydrogels to diverse non-porous surfaces. *Nature Materials*. [DOI: 10.1038/nmat4463](https://doi.org/10.1038/nmat4463).

Further Reading

[Inkjet Technique](#)

[Lithium-Ion Battery Safety for Electric Vehicles](#)

[Measuring the Surface Roughness](#)

[Contamination Analysis of Lithium-Ion Batteries](#)

[Battery Recycling Using XRF](#)

[Lithium-Ion Battery Supply Chain](#)

About the Sponsor: Seeing is Solving

EVIDENT is Empowering Solutions Through Advanced Visualization

Formerly a wholly owned subsidiary of Olympus Corporation, Evident separated from Olympus in 2022 to become a standalone company.

Built on 100 years of innovative technology and a strong foundation of industry leadership, we are committed to developing new technologies and delivering world-class customer service. At Evident, we are guided by the scientific spirit—innovation and exploration are at the heart of what we do. Committed to making people's lives healthier, safer, and more fulfilling, we support our customers with solutions that solve their challenges and advance their work.

Evident's Micro Imaging Solutions division manufactures a comprehensive range of optical-technology-based systems—including microscopes and objectives, slide scanners, and cell culture solutions—for life science applications like research, education, clinical pathology, hematology, and IVF as well as nondestructive industrial applications.

Our Test and Measurement division manufactures precision nondestructive testing instruments ranging from video borescopes to phased array and eddy current flaw detectors and X-ray fluorescence analyzers for a wide variety of applications, including maintenance, manufacturing, and environment and natural resources. These products are widely used for quality control, inspection, and measurement.

Evident is a steadfast partner that balances expertise in advanced technologies with approachability, so customers know they can bring us their questions, and we'll be ready with innovative technologies and groundbreaking solutions that support and empower them. Evident is hard-working and laser-focused on the needs of its customers to create modern solutions that are globally available. No matter where you work or what your challenge is, Evident can help.

[Learn more about who they are.](#)